Spectroscopy of ^{13}C above the α threshold with $\alpha + {}^{9}$Be reactions at low energies

I. Lombardo,[3,*] D. Dell'Aquila,[1,2,4,†] G. Spadaccini,[1,2] G. Verde,[3,4] and M. Vigilante[1,2]
[1]*Dip. di Fisica "E. Pancini," Università di Napoli Federico II, Via Cintia, I-80126 Napoli, Italy*
[2]*INFN-Sezione di Napoli, Via Cintia, I-80126 Napoli, Italy*
[3]*INFN-Sezione di Catania, Via S. Sofia, I-95126 Catania, Italy*
[4]*Institut de Physique Nucleaire d'Orsay (IPNO), Rue G. Clemenceau, 91406, Orsay, France*

(Received 7 November 2017; published 22 March 2018)

In this work we reinvestigate the spectroscopy of ^{13}C at excitation energies larger than the α emission threshold ($E_x > 10.648$ MeV) by means of a comprehensive R-matrix fit of experimental data concerning $\alpha + {}^{9}$Be collisions at low energies. Owing to the analysis of many reaction channels in a broad energy range, we improved the current knowledge on the level scheme of ^{13}C, by contributing to remove uncertain J^{π} assignments for several states. Some tentative speculations on the existence of molecular bands associated to cluster structures in this nucleus are also discussed.

DOI: 10.1103/PhysRevC.97.034320

I. INTRODUCTION

The accurate knowledge of ^{12}C structure is one of the most important topics in modern nuclear physics. Recent discoveries on the structure of this nucleus [1–5] emphasize the role played by cluster effects [6–8], suggest the possible appearance of symmetries [2,9] and unusual shapes [10] and stimulate new speculations on the existence of a dilute α-particle gas or even of a Bose-Einstein condensation [11–13].

In this context, also the study of non-self-conjugate nuclei is of noticeable importance because of the role played by extra-nucleons in modifying the α cluster structure [14–22]. However, if compared to the case of self-conjugate nuclei, this type of experimental investigations is made difficult by the presence of nucleon-decay channels that are open at low energies and, in general, by the presence of a high-level density [23].

Recently, the study of the structure of ^{13}C [24–26] was the object of a renewed interest, with particular emphasis to the role played by the valence neutron in the stabilization (or in the modification) of 3α cluster structures. These effects are particularly important above the α emission threshold in ^{13}C (i.e., $E_x = 10.648$ MeV [27]). For example, Ref. [24] suggested that two alternate-parity rotational bands could be observed in ^{13}C, suggesting some missing or uncertain J^{π} assignments to be conveniently modified. From the slope of proposed rotational bands, a very large moment of inertia ($\frac{\hbar^2}{2\Im} \approx 180$–$190$ keV) is deduced, consistent with a linear chain structure for ^{13}C*. Hereafter, several theoretical calculations have been performed on ^{13}C structure, for example, by means of the antisymmetryzed molecular dynamics (AMD) [28], the generator coordinate method (GCM) [29], and the orthogonality condition (OCM) [30] models. The presence of a negative parity rotational band built on the $3/2^-_2$ state has been predicted by GCM calculations in Ref. [29]. According to this model, the rotational band built on the $3/2^-_2$ excited state has a well-developed obtuse triangle three-α structure; therefore, it seems that the extra-neutron plays the role of stabilizing this exotic shape against the bending motion of the three α centers [29]. More recently, the search for the analogous of the Hoyle state in ^{13}C has been performed in Ref. [30] in the framework of the OCM model. The structure of several $1/2^{\pm}$ states has been theoretically investigated, and spectroscopic factors for several ^{12}C+n and ^{9}Be + α configurations have been calculated [30].

Despite the strong theoretical efforts, experimental data on the structure of ^{13}C at excitation energies above the α emission threshold are quite fragmentary and often characterized by conflicting J^{π} assignments that prevent any firm conclusions on the structure of this nucleus. Possible reactions that can help to clarify the situation are the $\alpha + {}^{9}$Be elastic and inelastic resonant scattering [25,31–36], ^{9}Be(α,n)^{12}C reactions [37–39], n+^{12}C elastic and inelastic scattering [40–42] and transfer reactions, such as the ^{9}Be(^{6}Li,d)^{13}C* case [26,43,44]. A review of results concerning ^{13}C spectroscopy is reported in Ref. [27].

Among the various possible reactions, $\alpha + {}^{9}$Be scattering has been suggested to be one of the best ways to populate molecular states in ^{13}C [25] due to the well pronounced molecular structure of the ^{9}Be target nucleus [14,45]. In Ref. [32], the structure of ^{13}C in the $E_x \approx 13.3$–14.5 MeV range is explored, with this reaction, by performing a fit of experimental excitation functions at several angles with predictions based on the Blatt-Biedenharn formalism [46]. More recently, Freer *et al.* [25] studied ^{9}Be + ^{4}He elastic scattering in inverse kinematics. The R-matrix fit to one excitation function at $\theta_{cm} \approx 180^{\circ}$ allowed to revise the J^{π} assignments and the partial width values of several ^{13}C states in the $E_x \approx 13.3$–16.2 MeV range. In particular, no clear evidence of the $\frac{9}{2}^{\pm}$ members of the molecular bands suggested in Ref. [24] has been found.

To clarify these questions and to improve the spectroscopy of ^{13}C, we have investigated $\alpha + {}^{9}$Be nuclear reactions at

*ivano.lombardo@ct.infn.it
†dellaquila@na.infn.it

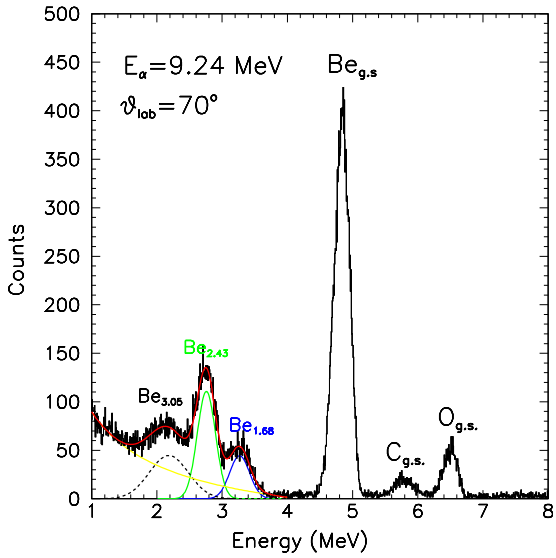

FIG. 1. Ejectile energy spectrum observed in $\alpha + {}^{9}$Be collisions at $E_\alpha = 9.24$ MeV and $\theta_{lab} = 70^\circ$. The small peaks at high energies are due to contaminants in the target. The group of peaks at 1.5–4 MeV is attributed to the inelastic scattering channels α_1 (^{9}Be at $E_x = 1.684$ MeV, blue line), α_2 (^{9}Be at $E_x = 2.429$ MeV, green line), and α_4 (^{9}Be at $E_x = 3.049$ MeV, black dashed line). The yellow line represents the assumed background. The red solid line shows the fit of inelastic peaks.

$E_\alpha \approx$ 1.5–10 MeV. A simultaneous R-matrix fit to elastic scattering (α_0) differential cross sections (DCS) obtained at several backward angles, inelastic scattering DCS leading to the first excited state (α_1, corresponding to $E_x = 1.684$ MeV) in ^{9}Be obtained at $\theta_{lab} = 70^\circ$, and integrated cross sections of ^{9}Be(α,n$_0$)^{12}C and ^{9}Be(α,n$_1$)^{12}C reactions allows us to estimate the spin and parity of several states above the α threshold, in a region where the existence of molecular bands is predicted. In Sec. II we briefly discuss the body of experimental data, while in Sec. III we discuss in details results obtained by a R-matrix fit of data, in connection with previous findings reported in the literature. In Sec. IV we compare our new results with theoretical calculations supporting the existence of molecular bands in ^{13}C.

II. SELECTION OF REACTION DATA-SET

The largest part of data used in the present R-matrix analysis derives from an experiment performed by using the TTT3 tandem accelerator in Napoli, Italy [47–49]. Beams of doubly ionized ^{4}He bombarded a self-supporting ^{9}Be target (122 μg/cm^2 thick). The beam energy was varied in $\simeq$ 60 keV steps, covering the $E_\alpha \simeq 3.5-10$ MeV domain. The detection system was made by an array of collimated silicon detectors placed at various backward angles. With this apparatus, elastic scattering DCS have been measured at 160°, 150°, 135°, 110° in the laboratory frame. Further details of the experimental setup and of a subsequent thick target experiment that benchmarked the DCS absolute cross section scale can be found in Ref. [47]. As an example, a typical ejectile energy spectrum obtained at $E_\alpha = 9.24$ MeV and $\theta_{lab} = 70^\circ$ is reported in Fig. 1 as a black line histogram. The most intense peak is associated to the elastic scattering of α particles on ^{9}Be nuclei. The two small peaks at higher energies are due to scattering events on carbon and oxygen contaminants in the target, as discussed in Ref. [47].

The low-energy group of peaks ($E \approx$ 2–4 MeV) is attributed to inelastic scattering processes on ^{9}Be. The energy positions of peaks at $E \approx$ 3.3, 2.7, and 2.2 MeV agree with predictions based on kinematics and energy loss calculations for $\alpha + {}^{9}$Be inelastic scattering events, exciting the 1.684 (α_1), 2.429 (α_2), and 3.049 MeV (α_4) states of ^{9}Be. Contributions due to $\alpha + {}^{16}$O inelastic scattering to this part of the energy spectrum are ruled out because of kinematics, while contributions due to $\alpha + {}^{12}$C are expected to be observed up to $E \approx$ 2 MeV. Furthermore, we verified by simulations that α particles coming from the breakup of excited states in ^{9}Be have a negligible influence on the region of inelastic scattering peaks.

We deduced the yield of the ^{9}Be(α,α_1)^{9}Be$_{1.68}$ inelastic scattering channel by fitting the low energy part of the spectrum in Fig. 1. We assumed the presence of inelastic peaks (parametrized with Gaussian functions) due to the 1.684 (blue line), 2.429 (green line), and 3.049 MeV (dashed line) states in ^{9}Be, summed on a smoothly varying background (yellow line). Concerning inelastic scattering events populating the very broad state at 2.78 MeV in ^{9}Be, the limited energy resolution makes it very difficult to distinguish them in the present analysis. After all, according to the NNDC database [50], this state was never observed in inelastic scattering collisions of α particles on ^{9}Be. The result of the fit procedure is reported in Fig. 1 as a red solid line. With this procedure, we succeeded in measuring DCS for the ^{9}Be(α,α_1)^{9}Be$_{1.68}$ inelastic scattering. It is also possible to estimate DCS for ^{9}Be(α,α_2)^{9}Be$_{2.43}$ and ^{9}Be(α,α_4)^{9}Be$_{3.05}$ inelastic channels, but because of the possible contamination due to the 2.78 MeV state, they have not been included in the present fit procedure. Uncertainties in elastic scattering DCS are taken from Ref. [47], while for inelastic scattering we evaluated uncertainties by square summing statistical and nonstatistical errors.

Since low energy states can interfere with higher energy states changing the shape of excitation functions [51], we complemented our elastic scattering DCS data-set with data at $\theta_{cm} = 160, 150^\circ$ taken from Ref. [33] and covering the energy range E$_\alpha \simeq$ 1.0–1.7 MeV. During the R-matrix fit procedure, we allowed the presence of small normalization factors (within 15% from unity) to account for eventual absolute normalization errors in the original data set of Ref. [33].

Regarding ^{9}Be(α,n)^{12}C reactions, we used absolute integrated cross-section data for the n_0 (i.e., associated with the reaction having ^{12}C in the ground state) and n_1 (i.e., having ^{12}C in the 4.44 MeV state) channels taken from Ref. [52] for the energy range E$_\alpha \simeq$ 1.4–3.5 MeV, and from Ref. [53,54] for the energy range E$_\alpha \simeq$ 2–7.5 MeV. Concerning the n_0 channel, the two data sets of Refs. [52–54] are in reasonable agreement in their overlap region, while for the n_1 channel a disagreement in the absolute cross-section scales is seen. Since the data concerning the total neutron cross section of Ref. [52] are in good agreement with the independent measurement of Ref. [55], we decided to use the cross-section scale of Ref. [52] as a reference for the n_1 channel. Anyway, if we normalize by a 0.52 factor the n_1 data of Refs. [53,54], they show a good

TABLE I. ^{13}C level structure derived from the R-matrix best-fit of ^{4}He + ^{9}Be elastic and inelastic scattering data and ^{9}Be$(\alpha,n)^{12}$C reactions. First two columns: summary of literature data, published before 1990, as reported in Ref. [27]. Third, fourth, and fifth columns: E_x, J^π, and $\Gamma_{\rm tot}$ values of ^{13}C excited states as obtained in the present work. Sixth, seventh, and eighth columns: Γ_{α_0}, Γ_{α_1}, and Γ_n partial width values obtained in the present work, rounded to 1 keV. Ninth column: references to states already reported in the literature. A cumulative maximum uncertainty of ≈20 keV is attributed to the energy position of states at $E_x < 14.3$ MeV and ≈50 keV at $E_x > 14.3$ MeV.

$E_x^{\rm lit}$	$J^\pi_{\rm lit}$	E_x	J^π	Γ	Γ_{α_0}	Γ_{α_1}	Γ_n	Refs.
11.75	$3/2^-$	11.75	$3/2^-$	116(27)	3(1)	—	113(26)	[27]
11.97	$5/2^+$	11.97	$5/2^+$	152(38)	65(17)	—	87(21)	[27,33]
12.13	$5/2^-$	12.17	$5/2^-$	199(28)	28(7)	—	171(21)	[27]
12.14	$1/2^+$	12.33	$1/2^+$	230(37)	40(7)	—	190(30)	[27]
12.44	$7/2^-$	12.45	$7/2^-$	222(36)	16(2)	—	206(34)	[27,42]
13.28	$3/2^-$	13.05	$3/2^-$	546(112)	153(29)	—	393(83)	[25,27,32]
13.41	$9/2^-$	13.41	$9/2^-$	84(27)	21(7)	—	63(20)	[25,27,32]
13.57	$7/2^-$	13.49	$7/2^-$	417(116)	114(51)	—	303(65)	[25,27]
13.76	$(3/2,5/2)^+$	13.63	$5/2^+$	743(51)	623(30)	—	120(21)	[26,27,32]
14.13	$3/2^-$	14.13	$5/2^-$	94(12)	94(12)	—	—	[25,27,32]
		14.17	$7/2^+$	6(1)	6(1)	—	—	[32]
14.39	$(1/2,5/2)^-$	14.28	$7/2^-$	392(93)	185(51)	—	207(42)	[25,27]
14.58	$(7/2^+,9/2^+)$	14.36	$9/2^+$	322(62)	70(16)	—	252(46)	[25–27]
14.98	$(7/2^-)$	14.64	$7/2^-$	361(47)	279(28)	—	82(19)	[27]
		15.04	$5/2^+$	965(377)	831(355)	—	134(22)	[27,38]
15.27	$9/2^+$	15.27	$3/2^+$	1201(280)	1061(260)	—	140(20)	[27,39]
16.08	$(7/2^+)$	16.09	$3/2^+$	365(55)	233(29)	55(14)	77(12)	[27]
		16.27	$5/2^-$	1596(142)	1503(130)	87(10)	6(2)	
16.18		16.40	$5/2^+$	17(4)	2(1)	14(2)	1(1)	[27]
		16.64	$5/2^-$	1502(156)	1294(110)	10(6)	153(40)	
		16.67	$7/2^+$	904(100)	633(100)	2(1)	—	
16.95		16.89	$9/2^+$	635(60)	501(40)	86(10)	4(2)	[27]
		16.91	$3/2^-$	1079(200)	702(100)	257(50)	120(50)	
		17.23	$3/2^+$	393(120)	280(80)	—	113(40)	
17.36		17.24	$3/2^-$	216(75)	185(60)	20(9)	11(6)	[27]
		17.52	$5/2^+$	2153(290)	1834(170)	86(50)	233(70)	
17.92		17.86	$7/2^-$	477(210)	457(200)	—	20(10)	[27]

agreement with the ones of Ref. [52] in the region of energy overlap (i.e., $E_\alpha \approx 1.84-3$ MeV). Therefore, we adopted such normalization factor for the n_1 data of Refs. [53,54]. We do not include data on the n_2 channel reported in Refs. [53,54] in the fit procedure. Indeed, its structureless trend seems to point out to a prominent direct mechanism, difficult to be reproduced with the R-matrix approach. Furthermore, its contribution is relatively minor as compared to the n_0 and n_1 channels. Finally, analogously to the n_1 case, normalization problems can affect the cross section scale. New accurate measurements of this reaction channel in a broad energy range would be very useful for future improvements of the present analysis.

III. RESULTS OF R-MATRIX FIT TO EXPERIMENTAL DATA

We performed a comprehensive R-matrix fit to the experimental data sets described in Sec. II. In the present analysis we used the multichannel, multilevel R-matrix code AZURE2 [51,56]. Similar results are obtained if a different R-matrix code is used ($minRmatrix$ code [23]). The maximum order of partial waves contributing to the reaction or scattering events was set to $\ell = 8$. The channel radii used in the R-matrix calculation are obtained by means of the formula $R = 1.4 \times (A_1^{1/3} + A_2^{1/3})$, with A_1 and A_2 being the mass numbers of the two particles constituting the reaction channel. Concerning the DCS measured in the Naples experiment, we included within the fit procedure the effects induced by the finite target thickness, as implemented into AZURE2 [56]; for this reason, the energy scale of DCS obtained from the Naples experiment here reported is directly derived from the bombarding energy.

As starting parameters of the fit procedure we used the table of states reported in Ref. [27], updated with the more recent findings described in Ref. [25]. The latter were obtained from an R-matrix analysis of α + ^{9}Be elastic scattering cross section measured with the thick target inverse kinematic method at $\theta_{\rm cm} \approx 180^\circ$. The presence of several angles and a wide energy range of elastic scattering DCS and the inclusion of inelastic scattering and neutron reaction channels allows us to discriminate between conflicting J^π assignments reported in the literature. Furthermore, the large body of data here used allow us to unveil the presence of broad states that can be missed when only one reaction channel and data in small energy ranges are analyzed. When necessary, J^π assignments tentatively reported in the literature have been changed to describe in the best possible way all the details of excitations functions. Results of the best fit procedure are summarized in Table I, together with previous findings reported in the literature. Red

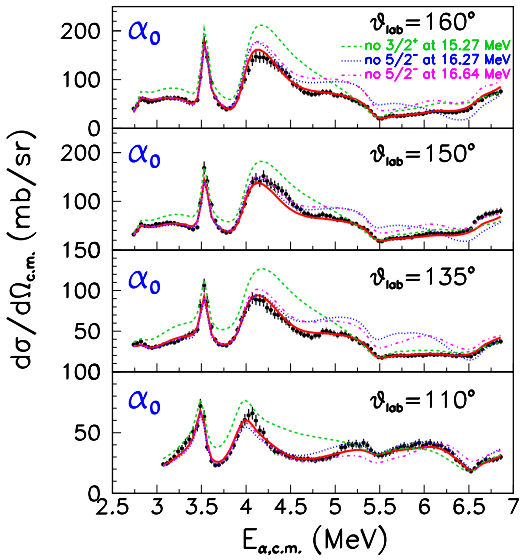

FIG. 2. ^{9}Be(α,α_0)^{9}Be DCS at laboratory angles of 160°, 150°, 135°, and 110°. Data are taken from Ref. [47]. The energy scale shown here represents the center of mass energy calculated starting from the α-particle bombarding energy. Effects of finite target thickness have been taken into account in the R-matrix fit. Red lines represent the results of the simultaneous multichannel R-matrix best-fit on the whole data set here investigated. Green dashed line: R-matrix best-fit without the $3/2^-$ state at 15.27 MeV. Blue dotted line: R-matrix best-fit without the $5/2^-$ state at 16.27 MeV. Magenta dash-dot line: R-matrix best-fit without the $5/2^-$ state at 16.64 MeV.

solid lines drawn in Figs. 2–8 of this article show the results of the best-fit procedure. The overall agreement with data is quite satisfactory, also in consideration of the high complexity of ^{13}C level scheme. Depending on the reaction channel, the reduced χ^2 ranges from ≈0.6 up to ≈2. Due to the complexity of the fit, uncertainties on the width parameters were estimated, as a first approximation, by finding a set of parameters describing in the best possible way the experimental data at the lower boundary of the 1σ confidence band. In the next subsections we discuss in more details the spectroscopic characteristics of excited states in ^{13}C as determined from the R-matrix fit procedure.

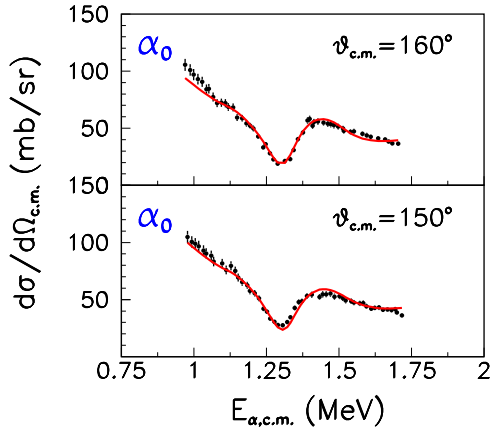

FIG. 3. Low-energy ^{9}Be(α,α_0)^{9}Be DCS at center of mass angles 160° and 150°. Data are taken from Ref. [33]. Red lines are the results of the R-matrix best-fit on the whole data set here investigated.

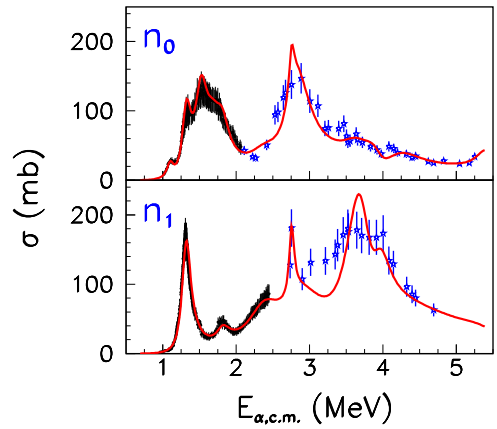

FIG. 4. Excitation functions of ^{9}Be(α,n$_0$)^{12}C$_{GS}$ and ^{9}Be(α,n$_1$)^{12}C$_{4.44}$ angle-integrated cross section. Black dots, data from Ref. [52]; blue stars, data from Refs. [53,54]. Average uncertainties of 15% have been used for both data sets. Red lines are the results of the simultaneous multichannel R-matrix fit on the whole data set here investigated.

A. Resonances in the E_{cm} = 1–2 MeV region

In the E_{cm} = 1–2 MeV region, the presence of excited states in ^{13}C leads to the appearance of a marked local minimum in the α_0 channel and to the presence of several peaks in the n_0 and n_1 neutron channels. The small peak seen at $E_{cm} \simeq 1.11$ MeV in the n_0 excitation function (see Fig. 4) is attributed to the presence of a $3/2^-$ state at 11.75 MeV, already seen in n + ^{12}C scattering experiment [27]. Reference [27] reports, for this state, a neutron branching ratio $\frac{\Gamma_n}{\Gamma_{tot}} = 0.80 \pm 0.08$ and a total width of 129 ± 40 keV. In our fit procedure, we find $\frac{\Gamma_{n_0}}{\Gamma_{tot}} =$

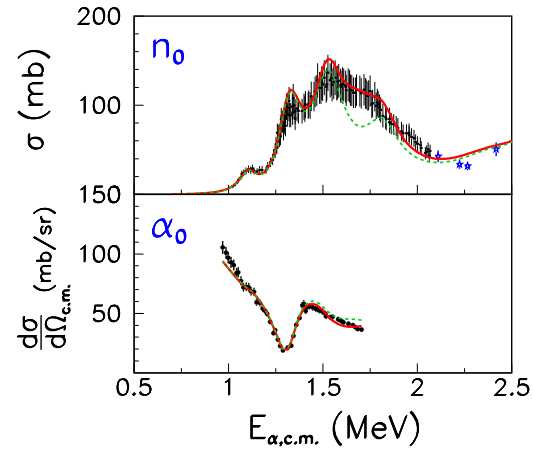

FIG. 5. (Upper panel) Zoom of ^{9}Be(α,n$_0$)^{12}C integrated cross-section data (see Fig. 4). Green dashed line: R-matrix best-fit without the inclusion of the $1/2^+$ state at 12.33 MeV. Red solid line: R-matrix best-fit with all the parameters of Table I. (Lower panel) The same of upper panel, but for the ^{9}Be(α,α_0)^{9}Be DCS at $\theta_{cm} = 160°$.

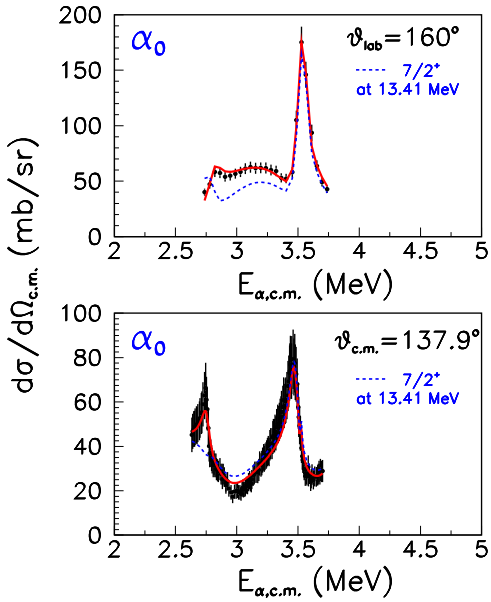

FIG. 6. (Upper panel) Zoom of ^{9}Be(α,α_0)^{9}Be DCS data at $\theta_{\rm lab} = 160^\circ$ (see Fig. 2). Blue dashed line: R-matrix best-fit where we changed the J^π value of the 13.41 MeV state from $9/2^-$ to $7/2^+$. Total and partial widths values used in the case of a $7/2^+$ assignment for the 13.41 MeV state are the same of those reported in Table I for the 13.41 MeV $9/2^-$ state. Red solid line: R-matrix best-fit with all the parameters of Table I. (lower panel) The same of upper panel, but for the ^{9}Be(α,α_0)^{9}Be DCS at $\theta_{\rm cm} = 137.9^\circ$. Data are taken from Ref. [32] and normalized as discussed in the text.

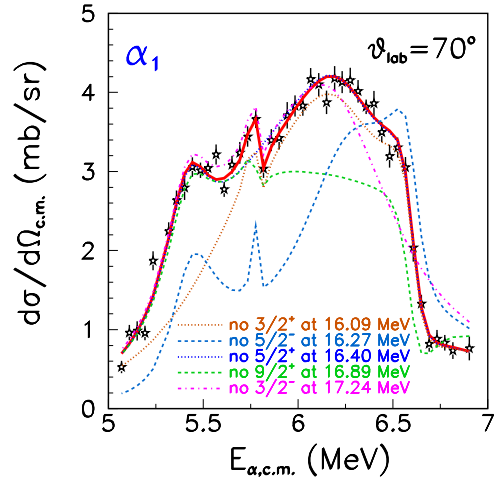

FIG. 7. ^{9}Be(α,α_1)^{9}Be$_{1.68}$ DCS data at $\theta_{\rm lab} = 70^\circ$. The red line represents the R-matrix best-fit on the whole data set here investigated. The brown dotted line is the R-matrix best-fit without the inclusion of the $3/2^+$ state at 16.09 MeV. The azure dashed line is the R-matrix best-fit without the inclusion of the $5/2^-$ state at 16.27 MeV. The blue dotted line is the R-matrix best-fit without the inclusion of the $5/2^+$ state at 16.40 MeV, responsible of the wing at $E_{\rm cm} \simeq 5.8$ MeV. The green dashed line is the R-matrix best-fit without the inclusion of the $9/2^+$ state at 16.89 MeV. Finally, the magenta dash-dot line is the R-matrix best-fit without the inclusion of the $3/2^-$ state at 17.24 MeV.

0.97 ± 0.01 and $\Gamma_{\rm tot} = 116 \pm 27$ keV, in reasonable agreement with the literature.

At $E_{\rm cm} \simeq 1.33$ MeV, both the n_0 and n_1 cross sections show a maximum (see Fig. 4), while the elastic channel shows a marked dip (see Fig. 5). In the literature, Saleh *et al.* [33] have attributed the dip in the elastic cross section to the effect of a $5/2^+$ state at 11.97 MeV. The presence of such a state was already reported in n + ^{12}C scattering experiments and in ^{9}Be(α,n)^{12}C reactions, even if with a tentative $7/2^-$ assignment in the latter case. We succeeded to fit well the data with a $5/2^+$ state at 11.97 MeV. Our total neutron branching ratio ($\frac{\Gamma_n}{\Gamma_{\rm tot}} \approx 0.57 \pm 0.09$) is in good agreement with the value quoted in the literature (0.51 ± 0.06 [27]). The width of this state (152 ± 38 keV) and the Γ_α partial width (65 ± 17 keV) are in agreement with the values reported in Ref. [33] (180 and 72 keV, respectively).

At $E_{\rm cm} \simeq 1.53$ MeV, the n_0 cross section shows a bump (Fig. 4) that has been attributed, in our analysis, to the presence of a $5/2^-$ state at 12.17 MeV. In this energy region, the literature reports four states (with different J^π and $\Gamma_{\rm tot}$ values) separated by just few tens of keV [27]. Among them, we can find also a $5/2^-$ state at 12.13 MeV, even if its total width (80 ± 30 keV) and neutron branching ratio (0.43 ± 0.06) are different from our estimates. Interestingly, in a more recent work, Wheldon *et al.* [26] measured with a refined coincidence technique the total width and branching ratios of this state, finding $\Gamma_{\rm tot}$=219 keV and $\frac{\Gamma_n}{\Gamma_{\rm tot}} \approx 1$, values compatible with the present ones.

At slightly higher energies, $E_{\rm cm} \simeq 1.79$ MeV, a shoulder appears on the n_0 excitation function. A good reproduction of data is achieved by including a $1/2^+$ excited state at 12.33 MeV having only α and n_0 branches. The effect of adding this state can be seen in Fig. 5, where the green dashed line shows the results of the best fit without including this state. We see a pronounced disagreement with the n_0 data, while the effect is

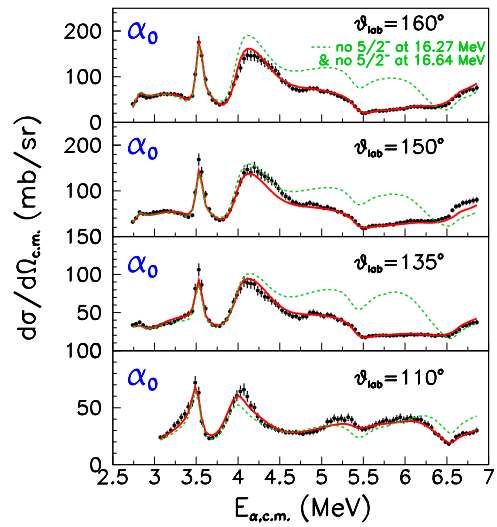

FIG. 8. ^{9}Be(α,α_0)^{9}Be DCS at laboratory angles of 160°, 150°, 135°, and 110°, as in Fig. 2. Red lines are the results of R-matrix best-fit. Green dashed lines represent the R-matrix best-fit without the inclusion of both the $5/2^-$ broad states at 16.27 and 16.64 MeV.

less evident in the elastic channel. A $1/2^+$ state at 12.14 MeV has been reported in the literature, even with a total with larger and a neutron branching ratio smaller than the present ones.

Finally, the last state contributing to this energy region is a $7/2^-$ at 12.45 MeV. It is responsible of the bump clearly visible in the ^{9}Be(α,n$_1$)^{12}C$_{4.44}$ excitation function at E$_{cm} \simeq$ 1.83 MeV (Fig. 4, bottom panel). The presence of a $7/2^-$ state at 12.43 MeV was reported in the literature [27]. The quoted total width (114 ± 40 keV, [27]) is not far from the present result (222 ± 36 keV), even if the neutron-decay branching ratio is lower than the present one. It is anyway interesting to underline that, in an older work studying the ^{12}C(n,n$'\gamma$)^{12}C$_{4.44}$ [42], a value $\Gamma_{tot} = 220$ keV was reported, in nice agreement with the present one.

B. Resonances in the E$_{cm}$ = 2–3 MeV region

This energy domain is mainly dominated by structureless shapes of $\alpha + ^9$Be elastic scattering DCS (see Ref. [32]). This fact, coupled to the use of the rarefied data points of Refs. [53,54] for the n_0 and n_1 channels, makes the spectroscopic investigation quite difficult. A broad $3/2^-$ 13.05 MeV state has to be included to reproduce the hole in the n_0 cross section around E$_{cm} \approx$ 2.4 MeV and to explain the corresponding shoulder in the n_1 channel at similar energies. The need to include a broad $3/2^-$ state at 13.28 MeV was pointed out by Ref. [32] and subsequently also in the more recent Ref. [25] by analyzing $\alpha + ^9$Be elastic scattering data. The total width obtained with the present R-matrix analysis (546 ± 112 keV) is larger than previous estimates of Refs. [25,32].

At E$_{cm} \simeq$ 2.76 MeV, a peculiar shape of α_0 and n_1 excitation function appears, as it can be seen in Figs. 2 and 4. By analyzing their $\alpha + ^9$Be elastic scattering data, Goss *et al.* [32] attributed this effect to the excitation of a high spin state (tentatively $9/2^-$) in ^{13}C at 13.41 MeV (with a $\Gamma_{tot} = 58$ keV). The presence of a resonance at this excitation energy with similar width was also reported in ^{12}C(n,n$'\gamma$)^{12}C$_{4.44}$ experiments [42]. In his more recent analysis, Freer *et al.* [25] included a $9/2^-$ state at 13.43 MeV, but with a width smaller than the present one. The authors also suggested that a $7/2^+$ assignment for this state could reproduce a resonance having ≈60 keV width at E$_{cm} \simeq$ 2.76 MeV, in agreement with the experimental data. Owing to the use of DCS at different angles, we can investigate this question in more detail. A satisfactory reproduction of elastic scattering DCS at all angles and of the narrow peak in the n_1 integrated cross section is obtained by including in the level scheme a $9/2^-$ state at 13.41 MeV, having $\Gamma_{tot} = 84 \pm 27$ keV, and branching ratios $\frac{\Gamma_{\alpha 0}}{\Gamma_{tot}} \approx 0.25$, $\frac{\Gamma_{n0}}{\Gamma_{tot}} \approx 0.29$, and $\frac{\Gamma_{n1}}{\Gamma_{tot}} \approx 0.46$. The α_0 and the $n_0 + n_1$ branching ratios quoted in Ref. [32] are in nice agreement with the present ones. Finally, we checked the possibility that the 13.41 MeV could have $7/2^+$ assignment. If we adopt such a J^π value for the state at 13.41 MeV, having Γ_{tot} and branching ratios equal to the previously mentioned ones, the associated R-matrix calculations are reported as blue dashed lines in Fig. 6. The disagreement with experimental DCS α_0 data at $\theta_{lab} = 160^\circ$ (upper panel) is evident. Similar disagreements are observed at the other angles here investigated. Furthermore, we analyzed also the very detailed data at $\theta_{cm} = 137.9^\circ$ (lower panel) reported in arbitrary units in Ref. [32]. They have been normalized so as to reproduce the R-matrix prediction for the peak at $E_{cm} \approx 3.5$ MeV. A very nice agreement between calculations and data is seen at $E_{cm} \approx 2.5$–3.0 MeV when using the $9/2^-$ assignment (red solid line), while the alternative assumption of a $7/2^+$ state at 13.41 MeV (blue dashed line) is in contrast with experimental data. We checked also the possibility that, in the case of a $7/2^+$ assignment, $\Gamma_{\alpha 0} > \Gamma_{n0}, \Gamma_{n1}$ with the constraint $\Gamma_{tot} = 84$ keV; also in this case calculations and experimental data for the α_0, n_0, and n_1 channels largely disagree. Therefore, from the present work, a $9/2^-$ assignment is deduced for the state at 13.41 MeV.

C. Resonances in the E$_{cm}$ = 3–3.75 MeV region

$\alpha + ^9$Be elastic scattering data in this energy region are characterized by a very broad bump (E$_{cm} \simeq$ 2.9−3.4 MeV), followed by a more narrow peak (E$_{cm} \simeq$ 3.5 MeV) and a broad local minimum (E$_{cm} \simeq$ 3.85 MeV), as clearly visible in Fig. 2. The evolution with the angle of the broad bump is very evident, and it is a useful tool to determine J^π values of states contributing in this energy region. We find that two broad states are needed to simultaneously reproduce the α_0, n_0, and n_1 excitation functions: a $7/2^-$ state at 13.49 MeV and a $5/2^+$ state at 13.64 MeV. Similar findings are reported by Freer *et al.* [25], even if the Γ_{tot} and the branching ratios values seem to be inverted between the two states. In particular, for the $7/2^-$ state, present data suggest a quite small α_0 branching ratio, even if a sizable portion of the Γ_{α_0} value is associated to the $\ell = 4$ partial wave.

A good reproduction of the α_0 channel data is seen at all the angles, and also a reasonable reproduction of the n_0 and n_1 channels is seen. Probably the small gap between data and fit in the n_1 channel could be reduced by taking into account also a nonzero branching to the n_2 reaction channel. In this energy region, Wheldon *et al.* [26] reported the presence of a state at 13.78 MeV having a quite narrow width (117 keV). According to Ref. [26], this state has sizable branches to the α_0 and n_1 channels. In principle, the presence of such a state can help to reduce the gap in the n_1 channel before mentioned, especially in the E$_{cm} \simeq$ 3.11 MeV region. The absence of a pronounced (and narrow) structure near this energy value in the α_0 channel data makes quite difficult to evince the presence of such a state from the present analysis.

Following the suggestions by Goss *et al.*, the peak at E$_{cm} \simeq$ 3.5 MeV has been reproduced by using two close-lying states at 14.13 MeV ($5/2^-$) and 14.17 MeV ($7/2^+$). Concerning the $5/2^-$ state, its Γ_{tot} value (94 ± 12 keV) is in reasonable agreement with the ones quoted by Goss *et al.* (75 keV) and Freer *et al.* (124 keV). Furthermore, a vanishingly small neutron width is observed in all the investigations. In agreement with Goss *et al.*, we found that the largest part of the α_0 width is due to the $\ell = 4$ partial wave. Concerning the $7/2^+$ state, as suggested by Goss *et al.*, we included it to reproduce the shape of the E$_{cm} \simeq$ 3.5 MeV peak at all angles. Anyway, we find a width much smaller than the Ref. [32] one.

The broad local minimum (E$_{cm} \simeq$ 3.75 MeV) seen in the α_0 excitation functions at all angles is due to the presence of a $7/2^-$ state at 14.27 MeV, interfering with the neighboring states and

with Coulomb background amplitudes. In Ref. [27], a negative parity state is reported at a close energy (14.39 MeV), with $J = 1/2$ or $5/2$ tentative assignments. In more recent times, a $7/2^-$ state at 14.4 MeV was reported in Ref. [25] but with a $\Gamma_{\rm tot}$ value quite smaller than the present one. Our value ($\Gamma_{\rm tot} = 392 \pm 93$ keV) agrees with the one quoted in Ref. [27] ($\Gamma_{\rm tot} = 280 \pm 70$ keV) within uncertainties.

D. Resonances in the $E_{cm} = 3.75-5.5$ MeV region

In this region the α_0 elastic scattering data show two very broad bump, and also some broad structures appear in the neutron channels. To simultaneously describe all the data, we used four (mainly broad) states. The first two ones are a $9/2^+$ state at 14.36 MeV and a $7/2^-$ state at 14.64 MeV (the last one with a dominant $\ell = 4$ component in the α_0 channel, $\theta_\alpha^2 \approx 0.47$). Two states with the same J^π assignments and similar $\Gamma_{\rm tot}$ values are reported in Ref. [25], even if our resonance energies are shifted back by ≈300 keV. Signals of the existence of a state near 14.63 MeV were reported in the study of $\alpha + {}^9$Be $\rightarrow$ $n_1 + {}^{12}$C* DCS [39]. In our investigations we find $\Gamma_{n_1} \gg \Gamma_{n_0}$, in qualitative agreement with the results of [39]. A state at 14.58 MeV ($\Gamma = 230$ keV) with uncertain J^π was reported in electron and proton inelastic scattering on ^{13}C [27]; in more recent times, the presence of a state near 14.58 MeV and with $\Gamma = 130$ keV was reported in Ref. [26]. We could assume that this state is related to the $7/2^-$ state at 14.64 MeV here observed; under this hypothesis, the branching ratios determined in the present work for the α_0, n_0, n_1 channels are similar to the ones determined in Ref. [26]. Finally, a narrow resonance having $\ell = 4$ has been observed at 14.7 MeV in ^{9}Be(^{6}Li,d)^{13}C transfer reactions [57,58]; also these findings could qualitatively support the existence of a $7/2^-$ state near the $\simeq$ 14.6 MeV region.

Two very broad states (a $5/2^+$ state at 15.04 MeV and a $3/2^+$ state at 15.27 MeV) are needed to reproduce the behavior of elastic scattering DCS in the region $E_{cm} \simeq 4-5.5$ MeV. The interference of these two states reproduces well the bump in the $E_{cm} \approx 4.7-5.4$ MeV region. The green dashed line of Fig. 2 shows the behavior of the R-matrix best fit if the $3/2^+$ state at 15.27 MeV is not included in the level scheme; the disagreement at all angles is evident. Both such states show large Γ_α partial width, but the associated reduced width γ_α^2 are well lower than the single-particle limits ($\ell = 3$, $\theta_\alpha^2 \simeq 0.33$ for the 15.04 MeV state and $\ell = 1$, $\theta_\alpha^2 \simeq 0.22$ for the 15.27 MeV state).

E. Resonances in the $E_{cm} = 5.5-6.8$ MeV region

In this high-energy region, α_0 DCS show a quite smooth behavior, with the exception of two pronounced dips at $E_{cm} \simeq 5.52$ MeV and $E_{cm} \simeq 6.5$ MeV. Also the α_1 channel shows some structures (e.g., a wing at $E_{cm} \simeq 5.8$ MeV) that are very useful to study the high energy part of ^{13}C level scheme. In this high-energy region, the spectroscopy of ^{13}C reported in the literature is particularly patchy [27]. Eleven states have been introduced in the present work to simultaneously fit all the reaction and scattering data here studied. For some states, we allowed the possibility of having nonzero strength in the α_2 inelastic channel.

The dip at $E_{cm} \simeq 5.52$ MeV is due to the 16.09 MeV $3/2^+$ state. In the literature, the presence of a state at $E_x \simeq 16.1$ MeV with $\Gamma_{\rm tot}$ of the order of 200–300 keV has been reported by analyzing both the ^{9}Be(α,n)^{12}C reaction and ^{12}C(n,n)^{12}C scattering data. The deep minimum, seen in the α_0 channel at $\theta_{\rm lab} = 110^\circ$ at $E_{cm} \simeq 6.51$ MeV, is due to the interferences between two close-lying states at 17.23 ($3/2^+$) and 17.24 ($3/2^-$) MeV. We verified this finding by removing them from the level list in the R-matrix calculation; in this case, the deep minimum is not reproduced at all.

The wing at $E_{cm} \simeq 5.8$ MeV in the α_1 inelastic channel can be attributed to a narrow $5/2^+$ state at 16.40 MeV. The blue dotted line of Fig. 7 represents the result of the R-matrix best-fit without the 16.40 MeV state: the wing in the excitation function disappears.

Apart from the presence of such dips and wings, the global behavior of α_0 and α_1 excitation functions in this energy region is determined by the contributions of four broad states ($\Gamma_{\rm tot} >$ 1 MeV). Their mutual interference and their interference with Coulomb amplitudes allow to describe the overall trend of data. In Fig. 2 we report, in different colours, the effect of removing some of these states from the R-matrix calculation. A much poorer agreement with data is seen in all cases. Furthermore, we checked the possibility that the two broad $5/2^-$ states at 16.27 and 16.64 MeV can balance out their effects. In Fig. 8 the green dashed line represents the present R-matrix best-fit without including both these states, and a strong disagreement with data is evident.

Because of the finite range of data, the spectroscopic information on the highest excitation states obtained with the present R-matrix analysis is not fully reliable. At bombarding energies larger than the ones here investigated, $E_\alpha > 10$ MeV, $\alpha + {}^9$Be elastic scattering DCS have been reported at several backward angles in Ref. [31]. The presence of broad resonant-like structures characterizes the DCS pattern up to $E_\alpha \approx 20$ MeV. Even if their nature was not definitely understood, they were attributed to direct reaction mechanisms, such as the optical model resonance phenomenon [31]. In this frame, it is also possible that the broad states appearing in the high excitation energy domain of our R-matrix analysis indicates the onset of such direct effects. New investigations of $\alpha + {}^9$Be reactions at high energies can help to better clarify this aspect.

IV. DISCUSSION ON ^{13}C ROTATIONAL BANDS

The broad body of spectroscopic data obtained in the present work allows us to draw some considerations on the structure of ^{13}C, in particular on the existence of molecular rotational bands. After the seminal work of Ref. [24], several results of theoretical calculations on the existence of molecular bands in ^{13}C were published [28,29]. Efforts have been made also to calculate the Γ_α for molecular band states within the WKB approach [59] and to determine the spectroscopic factors for $1/2^\pm$ states [30].

As a first point, we fix our attention to negative parity states on the light of the proposed molecular rotational band

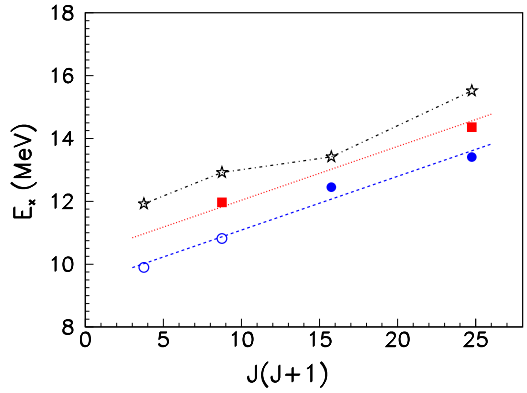

FIG. 9. States that could be involved in ^{13}C molecular bands. Black open stars: theoretical calculation of the negative parity band of ^{13}C built on the $3/2^-_2$ state, from Ref. [29]; the vertical scale has been transformed into excitation energy. Blue open circles: low-energy negative parity states suggested to belong to the $K^\pi = 3/2^-$ molecular band by Ref. [24]. Blue full circles: negative parity states seen in the present experiment and *naively* associated to the $K^\pi = 3/2^-$ molecular band. Blue dashed line: linear best fit of the four negative parity states. Red full squares: positive parity states that could *naively* belong to the $K^\pi = 3/2^+$ molecular band. The red dotted line has the same slope of the blue one, but it is shifted by $E_x = 0.95$ MeV; it is intended *only* to *guide the eye*.

of Ref. [24]. In our measurement we do not have access to the first two members of such a rotational band [$3/2^-$ at 9.897 MeV (subthreshold) and $5/2^-$ at 10.818 MeV]; at variance, we see well the contribution of the $7/2^-$ state at 12.45 MeV. For this state, we found a relatively small value of the dimensionless reduced α width $\theta^2_\alpha = \frac{\gamma^2_\alpha}{\gamma^2_{\alpha W}}$ ($\gamma^2_{\alpha W} = \frac{3\hbar^2}{2\mu R}$ is the Wigner single-particle limit), of the order of 0.05. Concerning the 14.13 MeV state, we discard the possibility, suggested in Ref. [24], to be a $9/2^-$ state. The $5/2^-$ assignment here reported, in agreement with Refs. [25,32], appears to be solid. Otherwise, a closer inspection of states in Table I, points out the presence of a $9/2^-$ state at 13.41 MeV. This state has a sizable dimensionless reduced α width ($\theta^2_\alpha = 0.21$) and we may suppose that it belongs to the negative parity molecular band. In this hypothesis, a reasonable fulfillment of the rotational band rule $E_x = \frac{\hbar^2 J(J+1)}{2\Im} + \text{const.}$ is seen, as shown by the blue dashed line in Fig. 9 (the coefficient of determination is $r^2 = 0.973$ in our hypothesis and $r^2 = 0.998$ for the suggested molecular band of Ref. [24]). It is interesting to note that, if our naive hypothesis was true, such a molecular band would have a slope coefficient $\frac{\hbar^2}{2\Im} \simeq 171$ keV. This value is very close to the one ($\frac{\hbar^2}{2\Im} \simeq 163$ keV) that can be extracted by a linear fit of theoretical data related to the $K^\pi = 3/2^-_2$ molecular band of Ref. [29]. The GCM model used in Ref. [29] suggests that the large value of the moment of inertia associated to the $K^\pi = 3/2^-_2$ band could be related to the presence of an obtuse-triangle configuration of the three α particles constituting the nuclear molecule. Being this hypothesis very intriguing, it certainly deserves further attentions both from experimental and theoretical points of view. Finally, contrary to the conjecture of Ref. [24], no evidence of high-energy states with $J^\pi = 11/2^-$ is seen in our work.

The situation is more complicated for positive parity states. Of all the states belonging to the positive parity molecular band of Ref. [24], only the $5/2^+$ level at 11.97 MeV is seen. This state has a sizable dimensionless reduced α width, $\theta^2_\alpha = 0.21$, and therefore it could have an α-cluster nature. A $9/2^+$ state ($\theta^2_\alpha \approx 0.05$) is reported at 14.36 MeV (see Table I). If we suppose that both such states belong to an hypothetical positive parity molecular band, a slope parameter $\frac{\hbar^2}{2\Im} \simeq 150$ keV is found, similar to the one reported for the negative parity band. If this naive hypothesis was true, the missing $7/2^+$ member would be at around 13 MeV, corresponding to $E_{\rm cm} \approx 2.35$ MeV. Indeed, the $E_{\rm cm} \approx 2$–2.5 MeV energy domain corresponds to a quite delicate region of the data set used for the present R-matrix analysis. This energy domain is at the matching between the two neutron data sets of Refs. [52,53].

Furthermore, if one looks at the $\alpha + {}^9$Be elastic scattering DCS from Refs. [32,34–36] (the only that cover this energy region), a structureless behavior is seen, making challenging the observation of (broad) states. New accurate measurements of $\alpha + {}^9$Be elastic scattering DCS and of ^{9}Be(α,n)^{12}C reaction cross sections in the energy region $E_\alpha \approx 2.0$–3.5 MeV are clearly required to improve the spectroscopic picture reported in the present work.

V. CONCLUSIONS

In this work we investigated the spectroscopy of ^{13}C at excitation energies larger than the α emission threshold ($E_x > 10.648$ MeV), an energy region where the onset of α-cluster phenomena is predicted by theoretical models [24,28–30]. A comprehensive R-matrix analysis of several reaction channels involving α and neutron emission has been performed. We simultaneously fit α_0 elastic scattering DCS data at four angles, α_1 inelastic scattering data and ^{9}Be(α,n$_0$)^{12}C, ^{9}Be(α,n$_1$)^{12}C reaction cross-section data. Owing to the analysis of many reaction channels in a broad energy range, we improved the current spectroscopic knowledge of excited states of ^{13}C, as reported in Table I. We made dedicated inspections when contrasting J^π assignments were reported in the literature for a given state. For example, our work confirms the $9/2^-$ assignment for the 13.41 MeV state and the $5/2^-$ assignment for the 14.13 MeV state, ruling out alternative choices suggested in Ref. [24] to explain the presence of molecular bands in such non self-conjugate nucleus.

Even if we are far from achieving definitive conclusions, our work reports a quite complete overview of ^{13}C spectroscopy at high excitation energies, and this leads us to make some (naive) speculations on the existence of exotic molecular shapes in this nucleus. In particular, if we attribute the $9/2^-$ state at 13.41 MeV to the negative-parity molecular band built on the $3/2^-_2$ state, we find a moment of inertia similar to the one theoretically predicted in Ref. [29] and associated to a bent three-α chain structure. At variance, from the present data, it is much more difficult to find evidence of the positive-parity molecular band. New experimental investigations of $\alpha + {}^9$Be reactions in the energy regions $E_\alpha \approx 2.0$–3.5 MeV and $E_\alpha > 10$ MeV can help to improve the presently reported

spectroscopy of ^{13}C and to clearly evidence the onset of direct processes in such reactions.

ACKNOWLEDGMENTS

We are indebted to R. J. De Boer (Notre Dame) and G. Rogachev (Texas A&M) for important discussions about the R-matrix theory and for making their R-matrix codes available to us. We thank E. Rosato (Napoli, *deceased*) for his support to the experimental and data analysis phases, and L. Campajola (Napoli) for the smooth running of the tandem accelerator during the experiment. We acknowledge gratefully C. Marchetta and E. Costa (INFN-Laboratori Nazionali del Sud, Catania) for manufacturing the ^{9}Be targets.

[1] M. Freer and H. O. U. Fynbo, Prog. Part. Nucl. Phys. **78**, 1 (2014).
[2] D. J. Marín-Lámbarri, R. Bijker, M. Freer, M. Gai, T. Kokalova, D. J. Parker, and C. Wheldon, Phys. Rev. Lett. **113**, 012502 (2014).
[3] W. R. Zimmerman, M. W. Ahmed, B. Bromberger, S. C. Stave, A. Breskin, V. Dangendorf, T. Delbar, M. Gai, S. S. Henshaw, J. M. Mueller, C. Sun, K. Tittelmeier, H. R. Weller, and Y. K. Wu, Phys. Rev. Lett. **110**, 152502 (2013).
[4] D. Dell'Aquila *et al.*, Phys. Rev. Lett. **119**, 132501 (2017).
[5] R. Smith, T. Kokalova, C. Wheldon, J. E. Bishop, M. Freer, N. Curtis, and D. J. Parker, Phys. Rev. Lett. **119**, 132502 (2017).
[6] C. Beck (Ed.), Lect. Notes Phys. **818**, 1 (2010).
[7] C. Beck (Ed.), Lect. Notes Phys. **848**, 1 (2012).
[8] C. Beck (Ed.), Lect. Notes Phys. **875**, 1 (2014).
[9] R. Bijker and F. Iachello, Phys. Rev. C **61**, 067305 (2000).
[10] T. Suhara, Y. Funaki, B. Zhou, H. Horiuchi, and A. Tohsaki, Phys. Rev. Lett. **112**, 062501 (2014).
[11] A. Tohsaki, H. Horiuchi, P. Schuck, and G. Röpke, Phys. Rev. Lett. **87**, 192501 (2001).
[12] Y. Funaki, Phys. Rev. C **92**, 021302(R) (2015).
[13] A. Raduta *et al.*, Phys. Lett. B **705**, 65 (2011).
[14] W. Von Oertzen, M. Freer, and Y. Kanada-En'yo, Phys. Rep. **432**, 43 (2006).
[15] C. Spitaleri, S. M. R. Puglia, M. LaCognata, L. Lamia, S. Cherubini, A. Cvetinovic, G. D'Agata, M. Gulino, G. L. Guardo, I. Indelicato, R. G. Pizzone, G. G. Rapisarda, S. Romano, M. L. Sergi, R. Sparta, S. Tudisco, A. Tumino, M. G. DelSanto, N. Carlin, M. G. Munhoz, F. A. Souza, A. S. deToledo, A. Mukhamedzhanov, C. Broggini, A. Caciolli, R. Depalo, R. Menegazzo, V. Rigato, I. Lombardo, and D. DellAquila, Phys. Rev. C **95**, 035801 (2017).
[16] M. Freer, J. D. Malcolm, N. L. Achouri, N. I. Ashwood, D. W. Bardayan, S. M. Brown, W. N. Catford, K. A. Chipps, J. Cizewski, N. Curtis, K. L. Jones, T. Munoz-Britton, S. D. Pain, N. Soić, C. Wheldon, G. L. Wilson, and V. A. Ziman, Phys. Rev. C **90**, 054324 (2014).
[17] N. I. Ashwood, N. M. Clarke, M. Freer, B. R. Fulton, R. J. Woolliscroft, W. N. Catford, V. A. Ziman, R. P. Ward, C. J. Bickerton, C. E. Harrison, and V. F. E. Pucknell, Phys. Rev. C **68**, 017603 (2003).
[18] H. Yamaguchi, D. Kahl, Y. Wakabayashi, S. Kubono, T. Hashimoto, S. Hayakawa, T. Kawabata, N. Iwasa, T. Teranishi, Y. K. Kwon, D. N. Binh, L. H. Khiem, and N. N. Duy, Phys. Rev. C **87**, 034303 (2013).
[19] V. Z. Goldberg and G. V. Rogachev, Phys. Rev. C **86**, 044314 (2012).
[20] D. Dell'Aquila *et al.*, EPJ Web Conf. **117**, 06011 (2016).
[21] D. Dell'Aquila, Nuovo Cimento C **39**, 272 (2016).
[22] D. Dell'Aquila, I. Lombardo, L. Acosta, R. Andolina, L. Auditore, G. Cardella, M. B. Chatterjiee, E. De Filippo, L. Francalanza, B. Gnoffo, G. Lanzalone, A. Pagano, E. V. Pagano, M. Papa, S. Pirrone, G. Politi, F. Porto, L. Quattrocchi, F. Rizzo, E. Rosato, P. Russotto, A. Trifirò, M. Trimarchi, G. Verde, and M. Vigilante, Phys. Rev. C **93**, 024611 (2016).
[23] M. L. Avila, G. V. Rogachev, V. Z. Goldberg, E. D. Johnson, K. W. Kemper, Y. M. Tchuvil'sky, and A. S. Volya, Phys. Rev. C **90**, 024327 (2014).
[24] M. Milin and W. von Oertzen, Eur. Phys. J. A **14**, 295 (2002).
[25] M. Freer, N. I. Ashwood, N. Curtis, A. Di Pietro, P. Figuera, M. Fisichella, L. Grassi, D. Jelavić Malenica, T. Kokalova, M. Koncul, T. Mijatović, M. Milin, L. Prepolec, V. Scuderi, N. Skukan, N. Soić, S. Szilner, V. Tokić, D. Torresi, and C. Wheldon, Phys. Rev. C **84**, 034317 (2011).
[26] C. Wheldon, N. I. Ashwood, M. Barr, N. Curtis, M. Freer, T. Kokalova, J. D. Malcolm, V. A. Ziman, T. Faestermann, H. F. Wirth, R. Hertenberger, and R. Lutter, Phys. Rev. C **86**, 044328 (2012).
[27] F. Ajzenberg-Selove, Nucl. Phys. A **523**, 1 (1991).
[28] Y. Chiba and M. Kimura, J. Phys. Conf. Ser. **569**, 012047 (2014).
[29] N. Furutachi and M. Kimura, Phys. Rev. C **83**, 021303(R) (2011).
[30] T. Yamada and Y. Funaki, Phys. Rev. C **92**, 034326 (2015).
[31] R. B. Taylor, N. R. Fletcher, and R. H. Davis, Nucl. Phys. **65**, 318 (1965).
[32] J. D. Goss *et al.*, Phys. Rev. C **7**, 1837 (1973).
[33] Z. A. Saleh *et al.*, Ann. Phys. **486**, 76 (1974).
[34] J. Leavitt *et al.*, Nucl. Instrum. Methods Phys. Res. B **85**, 37 (1994).
[35] J. Liu, Z. Zheng, and W. K. Chu, Nucl. Instrum. Methods Phys. Res. B **108**, 247 (1996).
[36] M. Zadro *et al.*, Nucl. Instrum. Methods Phys. Res. B **259**, 836 (2007).
[37] A. W. Obst, T. B. Grandy, and J. L. Weil, Phys. Rev. C **5**, 738 (1972).
[38] D. C. De Martini, C. R. Soltesz, and T. R. Donoghue, Phys. Rev. C **7**, 1824 (1973).
[39] D. E. Groce and B. D. Sowerby, Nature **206**, 494 (1965).
[40] H. D. Knox and R. O. Lane, Nucl. Phys. A **378**, 503 (1982).
[41] W. Tornow, J. Phys. G **9**, 1507 (1983).
[42] H. E. Hall and T. W. Bonner, Nucl. Phys. **14**, 295 (1959).
[43] X. Aslanoglou, K. W. Kemper, P. C. Farina, and D. E. Trcka, Phys. Rev. C **40**, 73 (1989).
[44] T. Kawabata *et al.*, J. Phys. Conf. Ser. **111**, 012013 (2008).
[45] D. Vinciguerra and T. Stovall, Nucl. Phys. A **132**, 410 (1969).
[46] J. M. Blatt and L. C. Biedenharn, Rev. Mod. Phys. **24**, 258 (1952).

[47] I. Lombardo *et al.*, Nucl. Instrum. Methods Phys. Res. B **302**, 19 (2013).
[48] I. Lombardo *et al.*, J. Phys. G: Nucl. Part. Phys. **40**, 125102 (2013).
[49] I. Lombardo *et al.*, J. Phys. G: Nucl. Part. Phys. **43**, 045109 (2016).
[50] Brookhaven National Laboratory, National Nuclear Data Center, http://www.nndc.bnl.gov/.
[51] M. Wiescher, R. J. deBoer, J. Görres, and R. E. Azuma, Phys. Rev. C **95**, 044617 (2017).
[52] R. Kunz, S. Barth, A. Denker, H. W. Drotleff, J. W. Hammer, H. Knee, and A. Mayer, Phys. Rev. C **53**, 2486 (1996).
[53] L. van der Zwan and K. W. Geiger, Nucl. Phys. A **152**, 481 (1970).
[54] K. W. Geiger and L. van der Zwan, Nucl. Instrum. Methods **131**, 315 (1975).
[55] P. R. Wrean, C. R. Brune, and R. W. Kavanagh, Phys. Rev. C **49**, 1205 (1994).
[56] R. E. Azuma, E. Uberseder, E. C. Simpson, C. R. Brune, H. Costantini, R. J. de Boer, J. Görres, M. Heil, P. J. LeBlanc, C. Ugalde, and M. Wiescher, Phys. Rev. C **81**, 045805 (2010).
[57] T. Borello-Lewin, Int. J. Mod. Phys. E **20**, 1018 (2011).
[58] M. R. D. Rodrigues, AIP Conf. Proc. **1351**, 125 (2011).
[59] J. C. Pei and F. R. Xu, Phys. Lett. B **650**, 224 (2007).